ELSEVIER

Structural Safety 22 (2000) 313–333

STRUCTURAL SAFETY

www.elsevier.nl/locate/strusafe

Structural reliability of concrete bridges including improved chloride-induced corrosion models

Kim Anh T. Vu, Mark G. Stewart *

Department of Civil, Surveying and Environmental Engineering, The University of Newcastle, Rankin Drive, Newcastle, NSW 2308, Australia

Abstract

A structural deterioration reliability (probabilistic) model has been used herein to calculate probabilities of structural failure. New reinforced concrete corrosion initiation, corrosion rate and time-variant load models are proposed. Three durability design specifications are considered in a lifetime reliability analysis of a RC slab bridge. Time-variant increases in loads are considered also. It was found that the application of de-icing salts causes significant long-term deterioration and reduction in structural safety for poor durability design specifications. A reduced cover or increased water-cement ratio increases failure probabilities. When compared to the case of "no deterioration", it was observed also that the probability of failure only marginally increased for good durability design specifications. The approaches described herein are relevant to other physical infrastructure also.

Keywords: Structural reliability; Deterioration; Corrosion; Reinforced concrete; Bridges

1. Introduction

Poor concrete durability and corrosion of reinforcement bars are the primary cause of structural deterioration of bridge decks, piers and other structures. Corrosion-initiated longitudinal cracking and associated spalling of the concrete cover are particularly common problems in concrete structures. Corrosion is initiated mainly by chloride contamination, often in conjunction with inadequate cover or poor quality concrete. Chlorides may diffuse through the protective concrete cover or corrosion may be initiated also by cracking. Reinforcement corrosion causes loss of area (metal loss) and the increased volume of corrosion products (rust) causes concrete tensile stresses that may be sufficiently large to cause internal microcracking, external longitudinal

* Corresponding author. Tel.: +61-2-4921-6027; fax: +61-2-4921-6991.
E-mail address: mark.stewart@newcastle.edu.au (M.G. Stewart).

0167-4730/00/$ - see front matter
PII: S0167-4730(00)00018-7

cracking and eventually spalling. This may lead to an acceleration in corrosion rate and/or reduction of bond — leading to serviceability failure and/or a loss of structural integrity.

The cost of maintaining, repairing or replacing degraded existing structures is immense [1]. Hence, there is obviously a strong financial incentive for the optimal allocation of resources, not only for repair and rehabilitation strategies, but also for initial design, construction and proposed maintenance of future structures in order to optimise life-cycle performance.

Reliability analysis includes probabilistic information from all resistance and loading variables influencing the assessment process (not just point estimates) and so provides a rational criterion for the comparison of the likely consequences of decisions taken under uncertainty. Hence, risk-based approaches clearly define "safety" or other performance criteria and provide a measure by which safety, cost-effectiveness and other management considerations can be measured or compared against. Existing Bridge Management Systems such as PONTIS are deterministic (point estimates) only and do not consider the functionality or load carrying capacity of a bridge [2]. It is for these reasons that the UK Highways Agency, amongst others, is developing reliability-based management systems for highway structures [3].

A structural deterioration life-cycle reliability (probabilistic) model is used herein to calculate probabilities of structural failure. This model is an extension of that proposed by Stewart and Rosowsky [4,5]; improvements include more accurate corrosion initiation and propagation models that include the effect of durability specifications on time-variant corrosion rates, a time-variant loading model and a shear failure limit state. For illustrative purposes only, the practical application of life-cycle reliability is applied to a typical reinforced concrete (RC) bridge. Chloride contamination can occur from (i) the application of de-icing salts and (ii) sea-spray (atmospheric marine zone). The influence of mix composition (water–cement ratio), cover and distance from the ocean (for sea-spray conditions) are also included in the analysis. Time-dependent probabilities of failure are then calculated for annual increments over the lifetime of the structure (100 years).

2. Improved deterioration model

2.1. Existing deterioration model [4,5]

The existing deterioration model developed by Stewart and Rosowsky [4,5] assumes:

- Chloride content [$C(x, t)$] at a distance x from the concrete surface at time t is

$$C(x, t) = C_o\left[1 - \mathrm{erf}\left(\frac{x}{2\sqrt{tD}}\right)\right] \tag{1}$$

  where C_o is the surface chloride content (kg/m^3 of concrete), D is the chloride diffusion coefficient (cm^2/sec) and erf is the error function.
- The influence of water-cement ratio on the diffusion coefficient (D) is obtained from a linear regression analysis of data described by Bentz et al. [6].
- Ordinary Portland Cement (OPC or Type I) used for all concrete mixes.

- The chloride concentration must reach a critical threshold chloride concentration (C_r) to cause dissolution of the protective passive film around the reinforcement, thereby initiating corrosion of reinforcement.
- Transverse crack width (intersecting cracks crossing the main reinforcement) caused by drying shrinkage or load-induced flexure will affect the initiation of corrosion, but corrosion is confined to the cracked zone and does not affect the subsequent propagation process.
- CEB-FIP Model Code [7] is used to predict the maximum crack width (w_{max}).
- Highly localised pitting of individual reinforcement bars is normally associated with chloride-induced corrosion. Given that pitting is spatially distributed it is unlikely that many bars will be affected by pitting; hence, pitting corrosion will not significantly influence structural capacity at any given cross-section of a RC slab. As such, the effects of pitting corrosion are not considered in the structural analysis.
- Transverse cracking will tend to result in highly localised corrosion, and as such will not cause longitudinal cracking or spalling.
- Chloride-induced (i.e. by chloride diffusion) corrosion will occur over a larger area (i.e. larger anode) and produce more uniform build up of corrosion products; thus resulting in longitudinal cracking and spalling.
- The model proposed by Liu and Weyers [8] is used to predict the time to longitudinal cracking and spalling.
- The corrosion rate is represented as a current density i_{corr} (normally expressed in $\mu A/cm^2$) where $\lambda \approx 0.0116 i_{corr}$ (mm/year). Corrosion of reinforcement will lead to a uniform reduction in the bar diameter of the reinforcing steel.
- Corrosion rate is not affected by concrete cover, water–cement ratio or longitudinal cracking and spalling.

Further details are provided in Stewart and Rosowsky [4,5] and limitations of this and other deterioration models are reviewed by Stewart [9]. The structural deterioration model is extended in the present paper to include (i) shear failure, (ii) effect of durability specifications on time to initiation, and (iii) effect of durability specifications on time-variant corrosion rates. Improvements to the corrosion initiation and propagation models are now described.

2.2. Improved corrosion initiation model

Numerous studies have found that the penetration of chlorides through concrete is best represented by a diffusion process if the concrete is assumed to be relatively moist. In this case, the penetration of chlorides is given empirically by Fick's second law of diffusion, see Eq. (1). However, field conditions differ significantly from that assumed with Fick's law (e.g. [5]). Nonetheless, Fick's law is often used to describe chloride penetration into concrete due to its computational convenience; namely, surface chloride concentration (C_o) and diffusion coefficients (D) are easily calculated by fitting Fick's law (''best fits'') to measured chloride profiles.

Nearly all chloride concentration data given in the literature refers to acid-soluble chloride concentrations. Hence, chloride concentrations used herein refer also to acid-soluble (or total) chlorides even though it is recognised that corrosion is influenced by the free (water-soluble) chloride concentration present in the concrete pore solution (e.g. [10]).

2.2.1. Surface chloride concentration — C_o

2.2.1.1. Application of de-icing salts. Exposure of concrete surfaces to de-icing salts arises from de-icing salts applied directly to the bridge deck or from traffic splash from roads [11]. Leaking from construction joints also contributes to increased surface chloride concentrations on bridge soffits, and the soffit is sheltered from rain so is less likely to be diluted by rain water. Middleton and Hogg [12] suggest that soffit and deck surface chloride concentrations are similar, and most reliability analyses assume this also. Given the scarcity of appropriate data, it is also assumed herein that soffit and deck surface chloride concentrations are identical.

A literature review has revealed a large number of data for surface chloride concentrations due to the application of de-icing salts (Fig. 1) for individual bridges or for groups of bridges (mean values). This data (as well as diffusion coefficients) are derived from curve-fitting to Fick's law assuming that the surface chloride concentration is in equilibrium with the concentration of chlorides in the saturated de-icing salt solution and so is constant with time (averaged over a year). The surface chloride concentration may be influenced by the amount of de-icing salts applied to a bridge deck (i.e. geographical location), efficiency of drainage, quality of expansion or construction joints, etc. This helps explain the high variability of surface chloride concentrations shown in Fig. 1. With reference to Fig. 1, it is observed that most of the data is below 5 kg/m^3.

The data described by Hoffman and Weyers [13] comprising samples taken from 321 concrete bridge decks in the US appears to be the most comprehensive to date and its mean of 3.5 kg/m^3 is in broad agreement with other data shown in Fig. 1. Thus, the mean and coefficient of variation

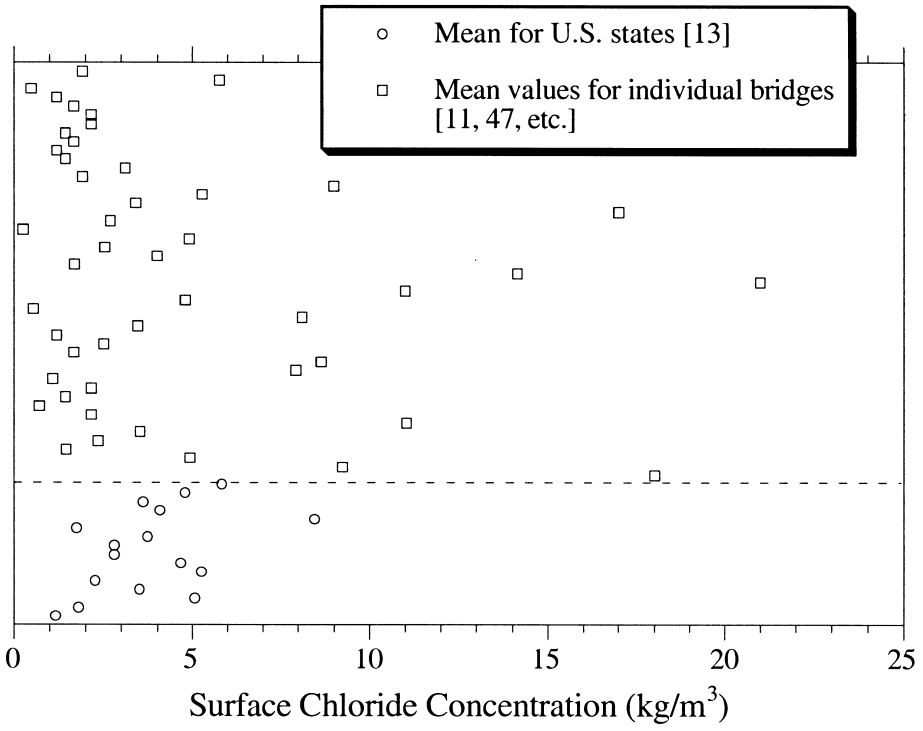

Fig. 1. Surface chloride concentrations for concrete exposed to de-icing salts.

of surface chloride content C_o (for the US) are 3.5 kg/m^3 and 0.5, respectively [13], and C_o is modelled by a lognormal distribution.

2.2.1.2. Coastal zone (sea-spray). In a coastal (atmospheric marine) zone, sea spray (water-borne chloride ions carried by the wind) will accumulate on the concrete surface. It is recognised that winds can carry sea spray over long distances inland, as much as 3 km or further (e.g. [14]). The concentration of air-borne chlorides on the surface of a concrete member is very much dependent on environmental conditions, topography, orientation of the concrete surface and distance from the coastline (e.g. [15]). It has been proposed that surface chloride content will increase with time in service (e.g. [16–18]). On the other hand, others suggest that surface chloride concentration is constant with time (e.g. [19,20]).

Unfortunately, the data for coastal atmospheric exposures is very limited; however, data reported by McGee [20] appears to be the most comprehensive study to date for bridges in atmospheric marine zones in a temperate climate. McGee [20] conducted a field-based study of 1158 bridges in the Australian state of Tasmania. In this study, McGee [20] suggests that the surface chloride concentration as a function of distance from the coast (d in km) is

$$\begin{aligned} C_o(d) &= 2.95 \text{ kg/m}^3 && d < 0.1 \text{ km} \\ C_o(d) &= 1.15 - 1.81 \cdot \log_{10}(d) && 0.1 \text{ km} < d < 2.84 \text{ km} \\ C_o(d) &= 0.03 \text{ kg/m}^3 && d > 2.84 \text{ km} \end{aligned} \tag{2}$$

McGee found that the coefficient of variation for surface chloride concentration was 0.49 for distances from the ocean exceeding 0.1 km. For the present study a coefficient of variation of 0.5 is used.

It has been found that the surface chloride concentration does not change significantly for heights above seawater levels exceeding 4 m [20,21]. Since most bridge decks are located in excess of 4 m above seawater levels it is assumed herein that height above seawater level is not an important consideration for this study.

2.2.2. Diffusion coefficient — D

The chloride diffusion coefficient (D) represents concrete permeability and is influenced by mix proportions (water–cement ratio, cement type), curing, compaction, environment (relative humidity and temperature) and time. The chloride diffusion coefficient is not significantly affected by the source of chlorides.

It has been observed that there is a tendency for a decrease in chloride diffusion coefficient with time (e.g. [21]), but that this reduction is most rapid during the first 5 years of exposure and after that approaches a constant value [19]. Bamforth and Price [19] also observed that there is very little time-dependent change in chloride diffusion coefficients for OPC. On the other hand, it is well accepted that water-cement ratio (mix proportion) has a significant influence on concrete permeability since an increase in water-cement ratio increases capillary porosity (e.g., [22]).

A number of models have been developed to consider the influence of mix proportions on chloride diffusion coefficient (e.g. [5,23–25]. All models exhibit similar trends (see Fig. 2) and for w/c ratios typical for most RC structures (0.35–0.5) differences between models are not significant. The model developed by Papadakis et al. [25] appears to be the best fit to the available literature, and is represented as

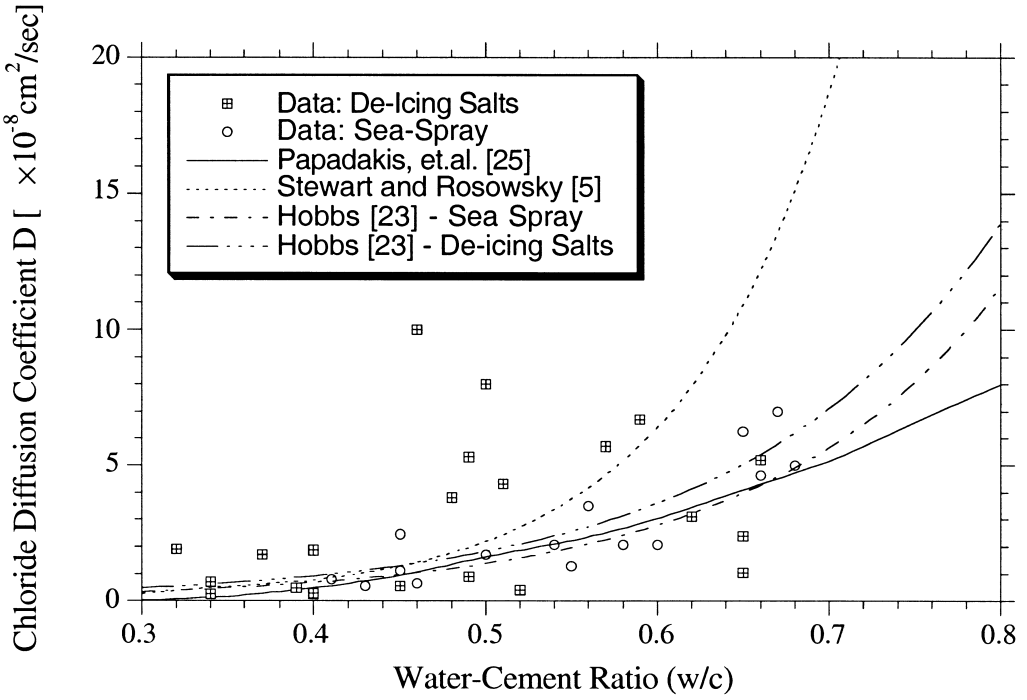

Fig. 2. Influence of water–cement ratio on diffusion coefficient.

$$D = D_{\mathrm{H_2O}} 0.15 \frac{1 + \rho_c \dfrac{c}{w}}{1 + \rho_c \dfrac{w}{c} + \dfrac{\rho_c}{\rho_a}\dfrac{a}{c}} \left(\frac{\rho_c \dfrac{w}{c} - 0.85}{1 + \rho_c \dfrac{w}{c}} \right)^3 \left(\mathrm{cm^2/s}\right) \tag{3}$$

where a/c is the aggregate-to-cement ratio, ρ_c and ρ_a are the mass densities of cement and aggregates respectively and D_{H_2O} is the chloride diffusion coefficient in an infinite solution ($=1.6\times10^{-5}$ cm^2/s for NaCl). The water-cement ratio is estimated from Bolomey's formula; namely,

$$w/c = \frac{27}{f'_{\mathrm{cyl}} + 13.5} \tag{4}$$

where f'_{cyl} is the concrete compressive strength of a standard test cylinder in MPa.

For a typical concrete compressive strength of 30–40 MPa the diffusion coefficient obtained from Eqs. (3) and (4) is approximately equal to 2.0E-8 cm^2/s and is consistent with a statistical analysis of bridge diffusion coefficients which found an overall US mean of approximately 2.0E-8 cm^2 [13]. If the specified (characteristic) compressive strength (F'_c) is specified by the designer (i.e. F'_c is known), then f'_{cyl} (see Table 2), w/c [Eq. (4)] and hence D [Eq. (3)] are dependent variables. Assuming no model error for Eq. (3), the coefficients of variation of diffusion coefficients derived from Eq. (3) for specified concrete compressive strengths of 30–40 MPa are approximately 0.45. Field-based studies have observed coefficients of variation of 0.5 for coastal structures [26], 0.69

for coastal structures [27] and 0.3–1.6 (mean = 0.75) for bridges in different states in the US [13]. The model predicted by Papadakis et al. [25] appears to be a reasonable fit to the data (see Fig. 2) so it is expected that the model error is not high. Unfortunately, existing data is of insufficient detail (e.g., a/c, ρ_c, ρ_a are unknown) to calculate accurately statistical parameters for the model error. As such, it is assumed herein that the mean and coefficients of variation for model error are 1.0 and 0.2, respectively.

2.2.2.1. Relationship between diffusion coefficient and surface chloride concentration. The previous discussion has assumed that the diffusion coefficient and surface chloride concentration are independently derived variables. This is not so. In nearly all reported data, diffusion coefficients and surface chloride concentrations are not obtained by physical measurements, but by "best fits" to Fick's law. However, there appears to be no correlation between these two parameters for the laboratory and field studies reported in the present paper.

2.3. Improved corrosion rate model

The corrosion rate will be governed by the availability of water and oxygen at the steel surface, and so is probably a function of concrete quality and cover. Unfortunately, information on the effects of such phenomena are limited. The electrical resistivity of the concrete is the governing factor when the ambient relative humidity is low. When relative humidity is high the oxygen availability at the cathode is the controlling factor affecting corrosion rate [10,28].

For many locations in Australia, US, Europe and Asia the average relative humidity is over 70% [10,29,30] and so it is assumed herein that the corrosion rate is limited by the availability of oxygen at the steel surface. As such, the oxygen availability depends on concrete quality (w/c ratio), cover and environmental conditions (temperature and relative humidity). The oxygen diffusion rate is calculated from Fick's first law of diffusion with the oxygen diffusion coefficient obtained from Tuutti [10]. The conversion of the oxygen diffusion rate to the corrosion rate is made considering the percentage of corrosion products and the molecular equations for corrosion reactions at the cathodic area [31]. The results of such calculations are shown in Fig. 3 which shows the effect of concrete quality and cover on the corrosion rate, for an ambient relative humidity of 75% and temperature of 20°C. For this typical environmental condition the influence of water–cement ratio and cover may be expressed empirically as

$$i_{corr}(1) = \frac{37.8(1 - w/c)^{-1.64}}{\text{cover}} \quad (\mu A/cm^2) \tag{5}$$

where $i_{corr}(1)$ is the corrosion rate at the start of corrosion propagation and cover is given in cm.

Most (if not all) reliability analyses have assumed that the corrosion rate is constant during the propagation period. However, it is expected that the formation of rust products on the steel surface will reduce the diffusion of the iron ions away from the steel surface. Also, the area ratio between the anode and cathode is reduced. This suggests that the corrosion rate will reduce with time; namely, rapidly during the first few years after initiation but then more slowly as it approaches a nearly uniform level [10,28,32]. Data reported by Liu and Weyers [32] is used herein to develop a relationship between time since initiation and the corrosion rate, which is expressed empirically as

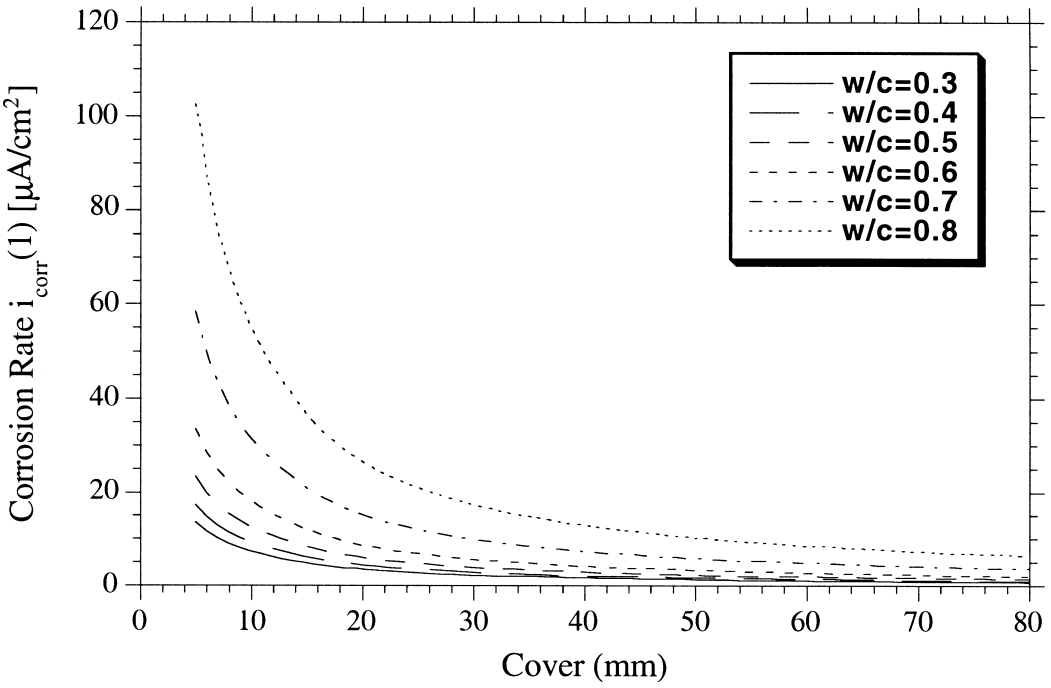

Fig. 3. Influence of water–cement ratio and cover on corrosion rate.

$$i_{corr}(t_P) = i_{corr}(1) \cdot 0.85 t_P^{-0.29} \tag{6}$$

where t_P is time since corrosion initiation and $i_{corr}(1)$ is given by Eq. (5) (see Fig. 4).

If the specified (characteristic) compressive strength ($F'c$) is specified by the designer, then f'_{cyl} (see Table 2), w/c [Eq. (4)] and hence corrosion rate [Eqs. (5) and (6)] are dependent variables. Assuming no model error, the coefficients of variation of corrosion rates derived from Eq. (5) for typical specified concrete compressive strengths of 30–40 MPa and 50 mm cover are approximately 0.25. In previous reliability studies, coefficients of variation varying from 0.14 to 0.33 have been used [33–35]. The corrosion rates predicted by Eq. (5) appear to be not unreasonable and within the range of typical corrosion rates found in the literature and so it is expected that the model error is not high. In the absence of any data to conduct a statistical analysis, it is assumed herein that the mean and coefficients of variation for model error are 1.0 and 0.2, respectively.

Fig. 5 shows the effect of the improved corrosion rate model on a reinforcing bar diameter, for 25 mm cover and various w/c ratios. It shows also that the time to corrosion initiation is influenced by the w/c ratio. [For this comparison, initiation due to shrinkage/flexural cracking is not considered.]. In general, existing uniform (linear) corrosion rate models (e.g. [4,5,33,34]) ignore the effect of concrete cover and water-cement ratio on corrosion rate and so tend to over-estimate the effects of corrosion for typical w/c ratios (less than 0.5). Hence, it is considered that the corrosion rate model proposed herein better represents the effects of durability specifications on corrosion.

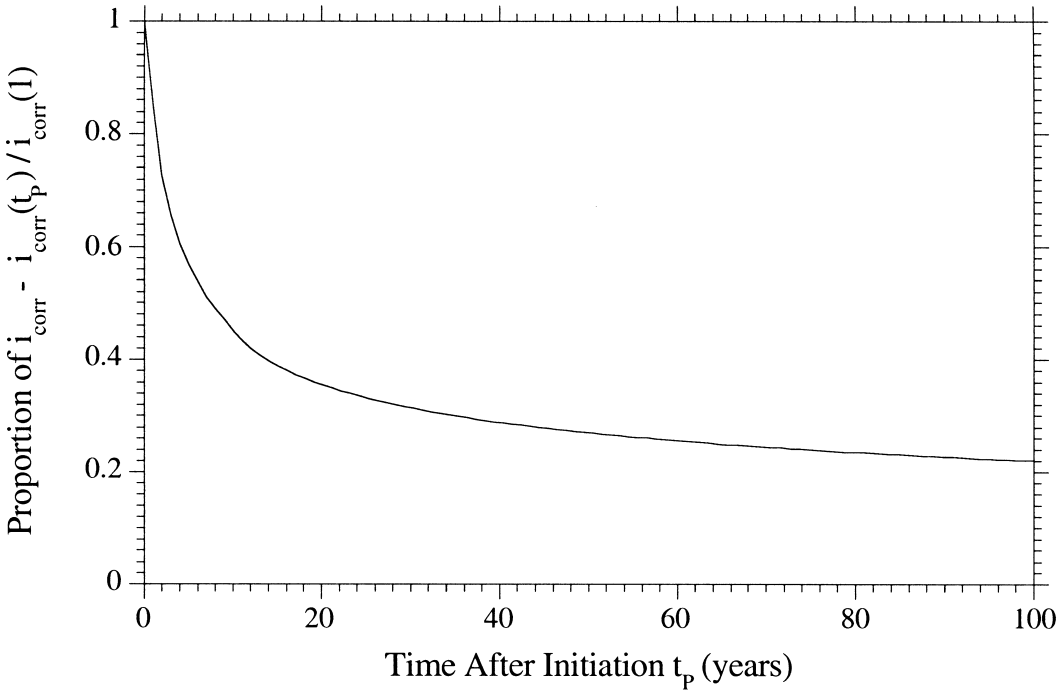

Fig. 4. Effect of time on corrosion rate.

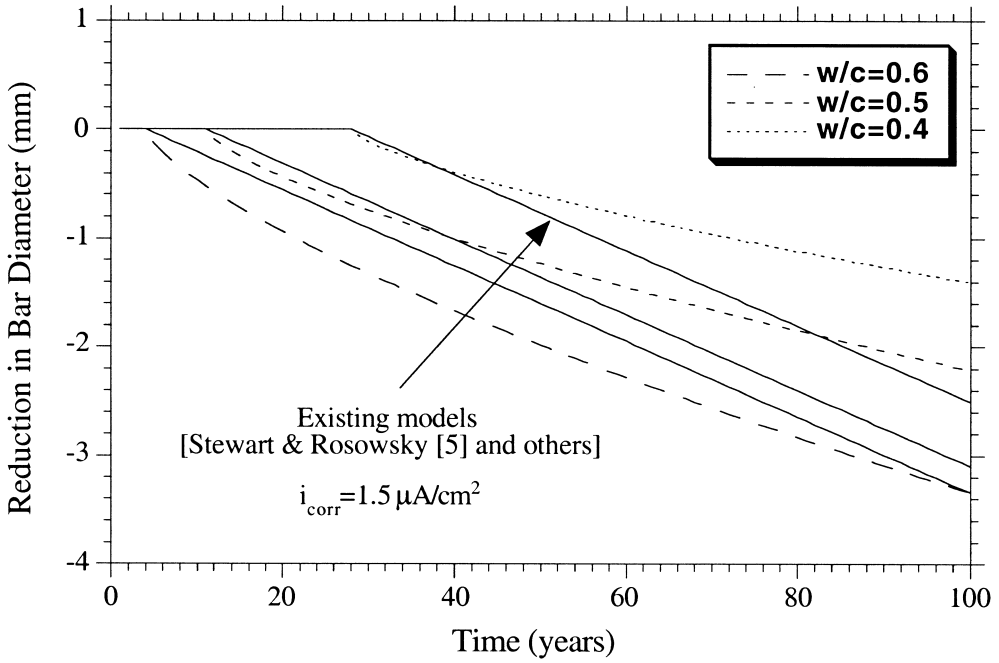

Fig. 5. Effect of improved corrosion rate model on bar diameter, for 25 mm concrete cover.

The proposed corrosion rate models are subject to limitations; mainly because they have been validated with few experimental data and most of this data is collected for relatively short periods of time. Nonetheless, these models have isolated the effect of important variables and so are useful for comparing the effect of durability design specifications and workmanship on structural performance and reliability.

Statistical parameters for corrosion variables are shown in Table 1. Note that statistical parameters for critical threshold chloride concentration (C_r), maximum crack width and critical crack width are the same as those reported by Stewart and Rosowsky [5].

2.4. Influence of spalling on structural strength

Corrosion-induced longitudinal cracking often leads to spalling or delamination. In such cases, experimental results suggest that structural capacity is reduced due to the concrete compression zone being reduced by the depth of the spalled/delaminated cover [36]. Hence, it is assumed herein that the onset of spalling of the top cover leads to delamination and so will reduce the effective depth of the concrete section by the top cover. For calculation of shear capacity, spalling of top or bottom cover will also lead to reduced section depth by one or both covers. However, reduction of bond is not considered herein as it appears that reduction of bond has a negligible effect on bridge reliability in flexure for typical corrosion rates [35].

A model proposed by Liu and Weyers [8] is used to predict the time to longitudinal cracking and spalling. In this model, time to longitudinal cracking and spalling is influenced by a large range of time-dependent and concrete strength dependent variables as well as time to initiation. This model is subject to considerable uncertainty. An experimental programme is currently underway at The University of Newcastle where recent experimental results suggest that this model may well under-estimate the actual time to spalling.

3. Time-dependent structural reliability

For structural assessment, the observation that a structure has actually survived is in itself a proof load and provides the assessor with some information about its structural capacity and

Table 1
Statistical parameters for corrosion variables

Parameter	Mean	Coefficient of variation	Distribution
D	Eq. (3)	–	–
Model error (D)	1.0	0.2	Normal
C_o — de-icing salts	3.5 kg/m^3	0.5	Lognormal
C_o — coastal zone	Eq. (2)	0.5	Lognormal
C_r	0.9 kg/m^3	0.19	Uniform (0.6–1.2)
i_{corr}	Eqs. (5) and (6)	–	–
Model error (i_{corr})	1.0	0.2	Uniform
w_{max}	1.0	0.4	Normal
Critical crack width	0.45 mm	0.19	Uniform (0.3–0.6)

safety (e.g. [37]). In other words this enables information about structural resistance to be updated. A revised or updated distribution of structural resistance can then be truncated at a known proof load or service loads may be treated as a proof load with uncertainty — resulting in the increase of bridge reliability for service proven (older) bridges (i.e. as survival age T increases). A significant increase in structural reliability occurs even if only normal or design service loads (plus dead load) are used to update structural reliability [38]; further increases will occur if abnormal events (e.g. grossly overloaded vehicles) are known.

In general, if it is assumed that n load events S_j occur within the time interval $(0, t_L)$ at times t_j $(j = 1, 2, ..., n)$, then the cumulative probability of failure of service proven structures (strength limit state) anytime during this time interval is (e.g. [39]):

$$p_f(t_L) = 1 - \Pr[R(t_1) > s_1 \cap R(t_2) > S_2 \cap ..... \cap R(t_n) > S_n] \qquad t_1 < t_2 < ... < t_n \leqslant t_L \tag{7}$$

where $R(t_1)$ represents the initial distribution of resistance and $R(t_2)$, $R(t_3)$, ..., $R(t_n)$ represent the structural resistances at time t_j updated on survival of the previous load events. It is evident that the updated structural resistances are influenced by the load history $S_1, S_2, ..., S_n$ as well as time-dependent changes in material properties. Thus, the cumulative probability of failure is dependent upon the prior and updated load and resistance histories. The above time-dependent reliability formulation can be extended to consider more realistic load realisations; namely, load combinations and stochastic load processes [40]. Monte-Carlo simulation analysis is used as the computational procedure [38].

3.1. Reference periods

The conditional probability that a bridge will fail in t subsequent years given that it has survived T years of loads is referred to herein as $p_f(t \mid T)$ and is expressed as

$$P_f(t \mid T) = [p_f(T + t) - p_f(T)]/[1 - p_f(T)] \tag{8}$$

where $p_f(T + t)$ and $p_f(T)$ are defined by Eq. (7). This conditional probability may also be referred to as a "hazard function".

Structural assessments are based on a limited reference period (normally 2–5 years) and at the end of this reference period the bridge should normally be re-assessed since after this period traffic conditions and structural capacity are likely to have changed beyond the accuracy of predictive models. Thus, it is more logical and accurate to compare probabilities of failure for relatively short reference periods.

3.2. Time-variant load model

For multiple-lane bridges the critical load effect generally occurs when heavily loaded trucks are side-by-side and have fully correlated weights [41]. Past experience suggests that traffic loads and volume will continue to increase. If (i) annual increases in trucks loads and heavy traffic (truck) volume are represented by λ_m and λ_v, respectively; (ii) number of crossings of heavily loaded fully correlated trucks per year is N, and (iii) truck weight is normally distributed, then the time-variant cumulative distribution of the weight of the heaviest truck w (annually) is

$$F_n(w, t) = \left[\Phi\left(\frac{w - \mu_w \bullet (1 + \lambda_m)^t}{\sigma_w \bullet (1 + \lambda_m)^t} \right) \right]^{N \bullet (1+\lambda_v)^t} \tag{9}$$

where t is time in years, μ_w and σ_w are statistical parameters of live load for a single truck and Φ is the cumulative function of the standard normal distribution. Annual maximum truck loads are assumed statistically independent.

It was considered that truck weights might be truncated at some upper physical limit, such as tyre or axle strength. The mean axle load (HS-20 truck) for a "heavily loaded truck" is approximately 55 kN [41]. However, experience suggests that individual axle loads have been measured (on a regular basis) at well over 200 kN in Australia and the US and that new designs and materials mean that some trucks will continue to carry loads well in excess of legal limits. Hence, it is considered not realistic to truncate probability distributions of present or anticipated truck weights.

4. Illustrative example

The following example will help illustrate the effect that durability design specifications can have on the time-dependent structural reliability for a "typical" RC slab bridge subject to the following adverse environments:

- exposed to repeated application of de-icing salts, or
- sited within 3km of the coast (atmospheric marine zone).

4.1. Structural configuration

The bridge considered in this study is a simply supported RC slab bridge with a span length of 10.7 m and a width of 14.2 m. The bridge was designed according to the AASHTO LRFD Bridge Design Specifications [42] for a HL-93 live load. Reinforcing steel is 400 MPa and there is a 75 mm thick bituminous overlay. The bridge design required a 550 mm thick slab with top and bottom reinforcement ratios of 0.1 and 0.8%, respectively. It is assumed that design (nominal) top and bottom covers (C_{tnom}, C_{bnom}) are equal. Three durability design specifications are considered:

- Poor: $F'_c = 25$ MPa, 25 mm cover.
- Fair: $F'_c = 40$ MPa, 50 mm cover.
- Good: $F'_c = 40$ MPa, 75 mm cover.

The number of design lanes for the bridge is three [42] and so the number of crossings of three fully correlated trucks (N) per year is approximately two [41]. Axle spacings and distribution of axle loads are based upon those of the standard HS-20 truck and these were used to calculate peak flexural and shear actions. Statistical parameters for dimensions, material properties, environmental conditions and loads appropriate for this RC concrete bridge are given in Table 2.

Table 2
Statistical parameters for resistance and loading variables

Parameter	Mean	COV	Distribution
Depth	$D_{nom} + 0.8$ mm	$\sigma = 3.6$ mm	Normal
C_{top}	$C_{tnom} + 19.8$ mm	$\sigma = 16.5$ mm	Normal
C_{bottom} [a]	$C_{bnom} + 8.6$ mm	$\sigma = 14.7$ mm	Normal
f'_{cyl}	F'_c [b] $+ 7.5$ MPa	$\sigma = 6$ MPa	Lognormal
k_w ($f'_c(28) = k_w f'_{cyl}$)	0.87	0.06	Normal
$f'_{ct}(t)$	$0.69\sqrt{f'_c(t)}$	0.2	Normal
$E_c(t)$	$4600\sqrt{f'_c(t)}$	0.12	Normal
f_{sy}	465 MPa	0.10	Beta
Humidity	0.75	0.05	Normal
Shear error	1.15	0.125	Normal
Flexure error	1.01	0.046	Normal
Dead load	$1.05D_n$	0.10	Normal
Asphalt	90 mm	0.25	Normal
Impact factor	1.15	0.10	Normal
Single truck live load	240 kN	0.40	Normal

[a] Truncated at 15 mm.
[b] F'_c, specified (characteristic) concrete compressive strength.

It is assumed that this is a low clearance bridge that passes over traffic lanes; hence it is likely that the slab soffit would also be exposed to de-icing salt chlorides from car spray at similar concentrations as the slab deck. For the atmospheric marine zone, both the deck and soffit are equally exposed to sea-spray.

In the reliability analysis "failure" is deemed to occur if the (i) bending moment exceeds the structural resistance at mid-span or (ii) shear capacity at the support is exceeded. Flexural and shear capacities are calculated from ACI318-1995 [43] requirements (most parameters being random variables) multiplied by the appropriate probabilistic model error (see Table 2). The time-dependent strength gain of concrete compressive strength, tensile strength and elastic modulus are included in the calculation of flexure and shear capacities. In this case,

$$f'_c(t) = \frac{t}{\lambda + \omega t} f'_c(28) \tag{10}$$

where t is the time in days, $\lambda = 4.0$ and $\omega = 0.85$ for moist cured normal (type I) Portland cement [44] and f'_c (28) is the 28-day concrete compressive strength. The concrete tensile strength (f'_{ct}) and elastic modulus (E_c) are dependent random variables (see Table 2).

4.2. Results

4.2.1. Structural resistance

Mean structural resistances as a function of time are shown in Figs. 6 and 7, for fair durability design specifications and all exposure conditions. In the present case, it is observed that corrosion can cause up to a 12% decrease in mean flexural resistance and a 5% decrease in mean shear

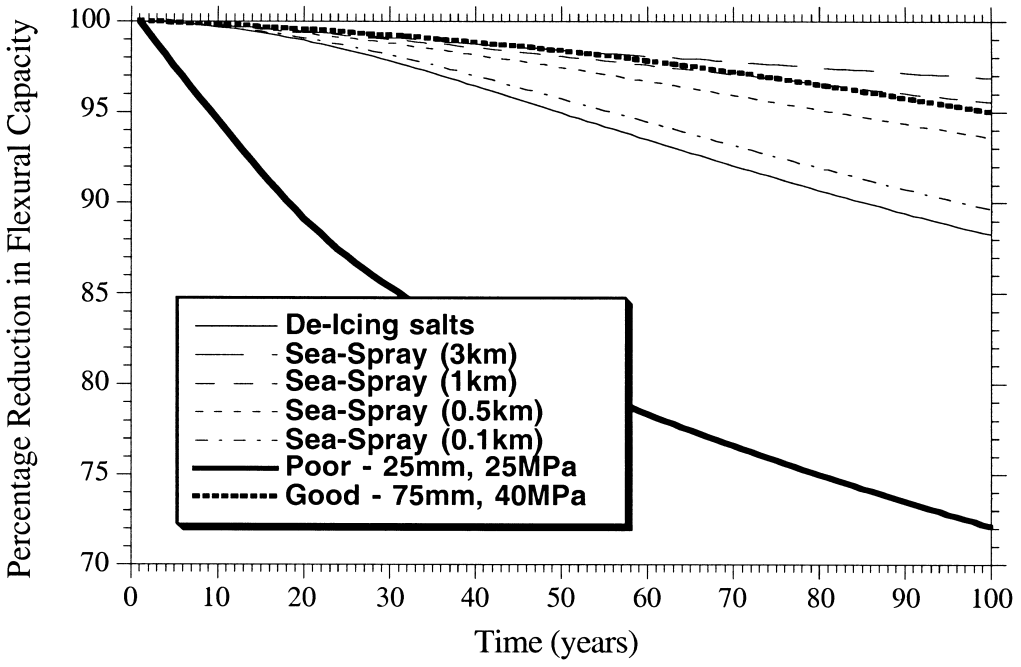

Fig. 6. Mean resistances for flexure.

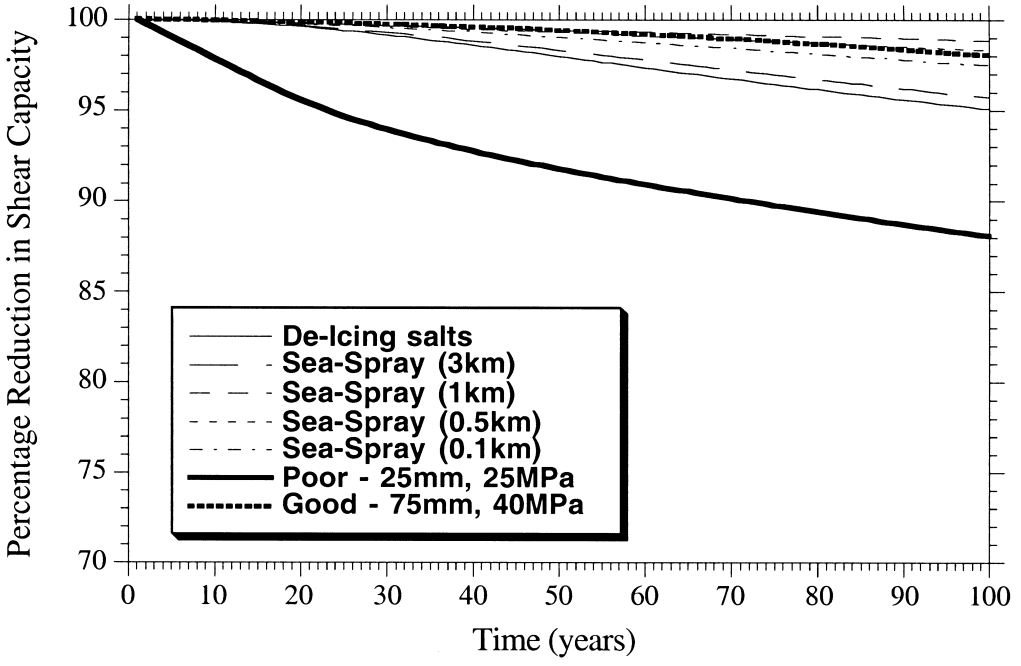

Fig. 7. Mean resistances for shear.

resistance for fair durability design specifications (de-icing salts). As a worst case scenario, a 30 and 12% decrease in flexural and shear capacities respectively is observed for a bridge with poor durability design specifications exposed to de-icing salts. Good durability specifications cause a minor decrease (less than 5%) in structural capacities. Bridges sited in excess of 1 km from the coast also experience negligible loss of structural capacity, for all durability design specifications.

Recall that in developing Figs. 6 and 7, it was assumed that spalling will lead to a reduced effective depth (e.g. loss of top cover compression zone). However, if it is assumed that spalling will not influence structural resistance in this manner (as has been the case with most previous reliability analyses including Stewart and Rosowsky [4,5]) then structural resistances shown in Figs. 6 and 7 would increase by only 10%.

4.2.2. Structural reliabilities

Fig. 8 shows cumulative probabilities of failure for all exposure conditions for a bridge designed to "fair" durability design specifications. Fig. 9 shows cumulative probabilities of failure for three durability design specifications (plus $F'_c = 25$ MPa, cover = 50 mm to compare the effect of cover and F'_c on structural reliability) and no deterioration. The cumulative (or lifetime) probability of failure is the probability that the structure will have failed anytime up to year t_L, [see Eq. (7)]. Differences between structural reliabilities for exposure to de-icing salts or sea-spray (0.1 km) are negligible, as is the difference between no deterioration and sea-spray (3 km) see (Fig. 8).

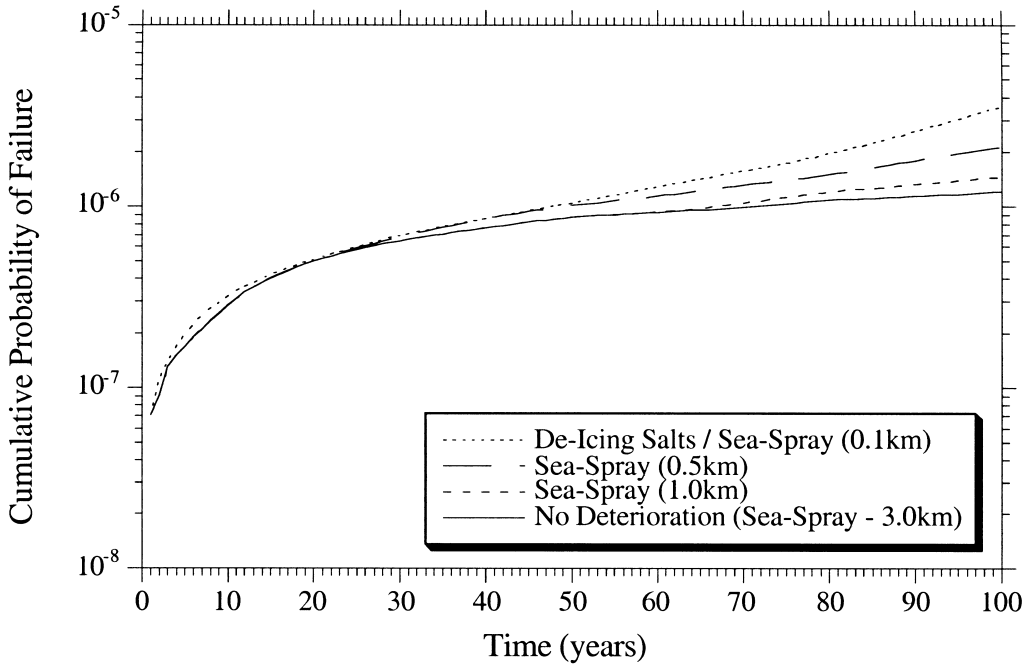

Fig. 8. Time-dependent cumulative probabilities of failure, for "fair" durability design specification.

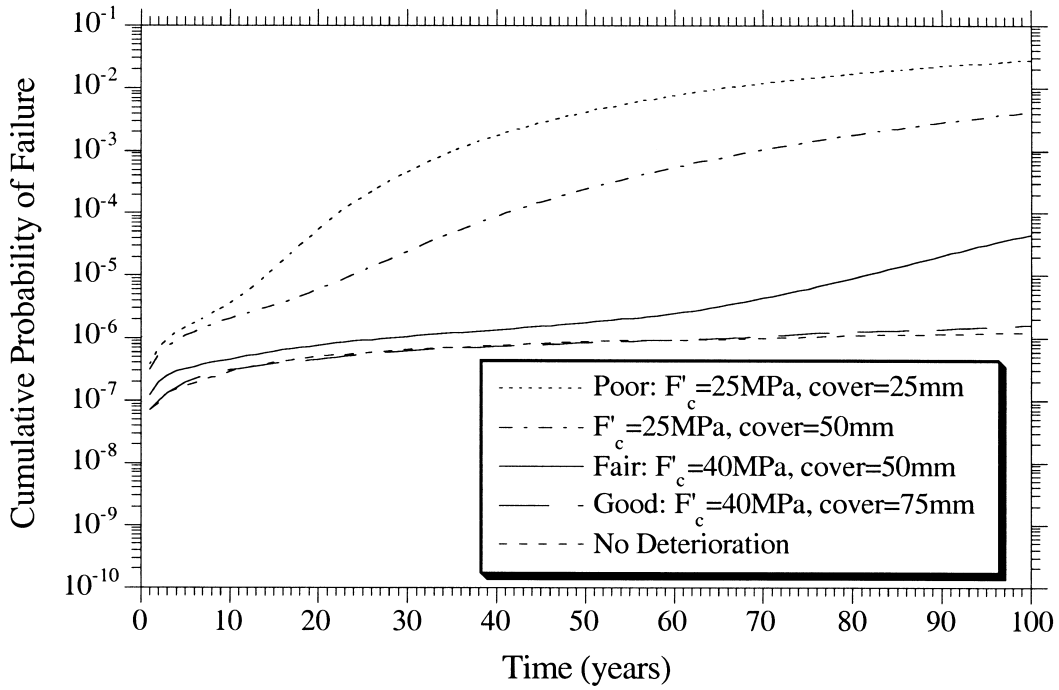

Fig. 9. Time-dependent cumulative probabilities of failure for de-icing salts and no deterioration.

It is observed from Fig. 9 that the probability of failure is only marginally increased for good durability design specifications (cf. no deterioration). Fig. 9 also shows the effect on structural reliabilities of designing the bridge to poorer durability design specifications. It is clear that lower standard durability specifications or poor construction workmanship will result in a dramatic increase in the risk of failure (by several orders of magnitude). For the cases considered herein, a reduction in concrete compressive strength (caused by an increase in the w/c ratio) is more detrimental to structural reliability than reduction in cover. This occurs because an increase in w/c ratio will increase the diffusion coefficient (and decrease time to initiation) and increase the corrosion rate (see Figs. 2 and 3) leading to corrosion, spalling and a greater time-dependent loss of structural capacity.

The present analysis ignores system effects such as collapse mechanisms and load redistribution; assumes all reinforcement corrodes uniformly across the entire bridge deck and assumes the absence of inspections and repairs (hence "failure" will occur whereas in practice signs of structural distress would indicate a need for repair) — this will necessarily lead to the overestimation of failure probabilities. It is clear that much scope exists for further work, although more accurate strength prediction models are available [45]. Hence, the structural reliabilities calculated in the present paper are still "notional" and so are used herein for comparative purposes only.

Based on Eq. (8), Fig. 10 shows the conditional (service proven) annual (reference period $t = 1$ year) probabilities of failure as a function of survival age T for no deterioration and the three durability design specifications. The conditional annual probability of failure is the probability of

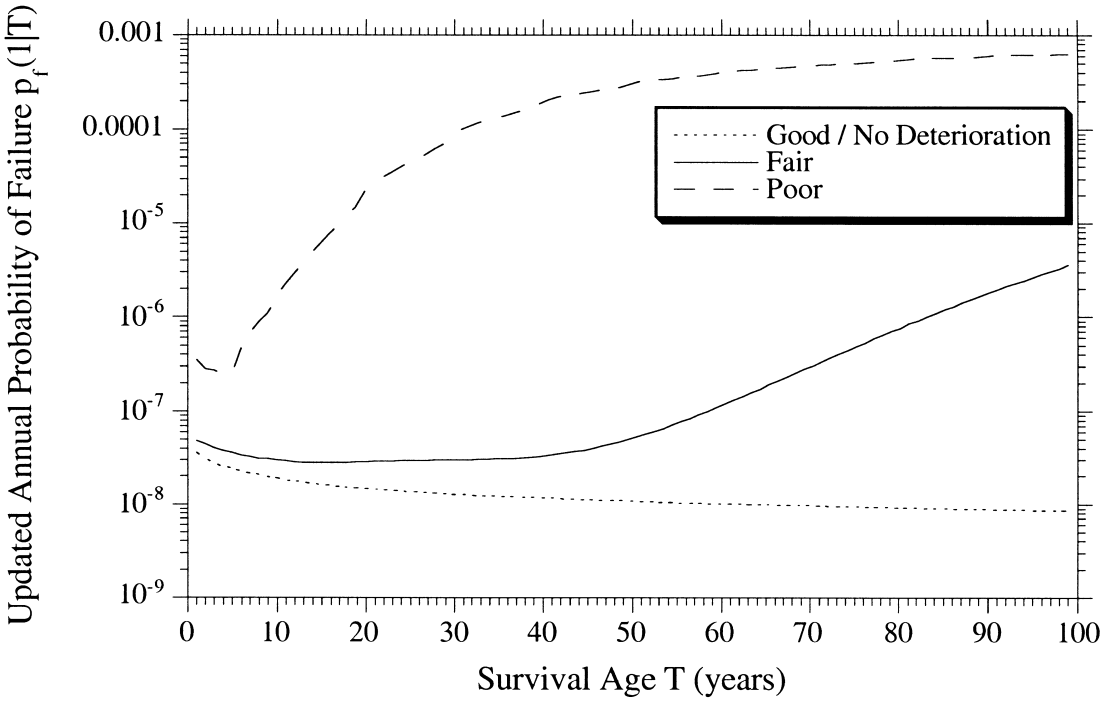

Fig. 10. Updated annual probabilities of failure for de-icing salts and no deterioration.

failure in year T. With reference to Fig. 10 note that initially the updated annual probability of failure reduces (due to beneficial effect of service proven performance) but then increases at later ages due to deterioration. If the reliability analysis does not include the effects of service-proven performance then this will result in an over-estimation of actual probabilities of failure.

For the bridge considered herein, the dominant mode of structural failure is shear for no deterioration; however, the proportion of flexural failures increases with time when the structure is exposed to aggressive environments. This is expected since loss of reinforcement area will have a more detrimental effect on flexural capacity (cf. Figs. 6 and 7). The proportion of flexural failures also increases as cover is reduced or water–cement ratio increased.

Fig. 11 shows the influence of moderate time-variant increases in truck loads and traffic volume, for no deterioration. It has been observed in the UK that the increase in heavy traffic (truck) volume matches very closely the annual growth in GDP [46]. For example, from 1950 to 1990, the average increase in GDP in the UK was 2.3%, hence λ_v is taken as 2.3%. For the sake of illustrative purposes, it is assumed that mean truck loads (λ_m) increase by 0.5% per annum (i.e. 65% increase in mean truck weights over next 100 years). For this loading scenario, it is noticed that probabilities of failure are not significantly affected for the first 20 years.

4.2.3. Sensitivity analysis

A sensitivity analysis was conducted to investigate the relative importance of the variability of each random variable on the variability of the flexural and shear strength limit state functions;

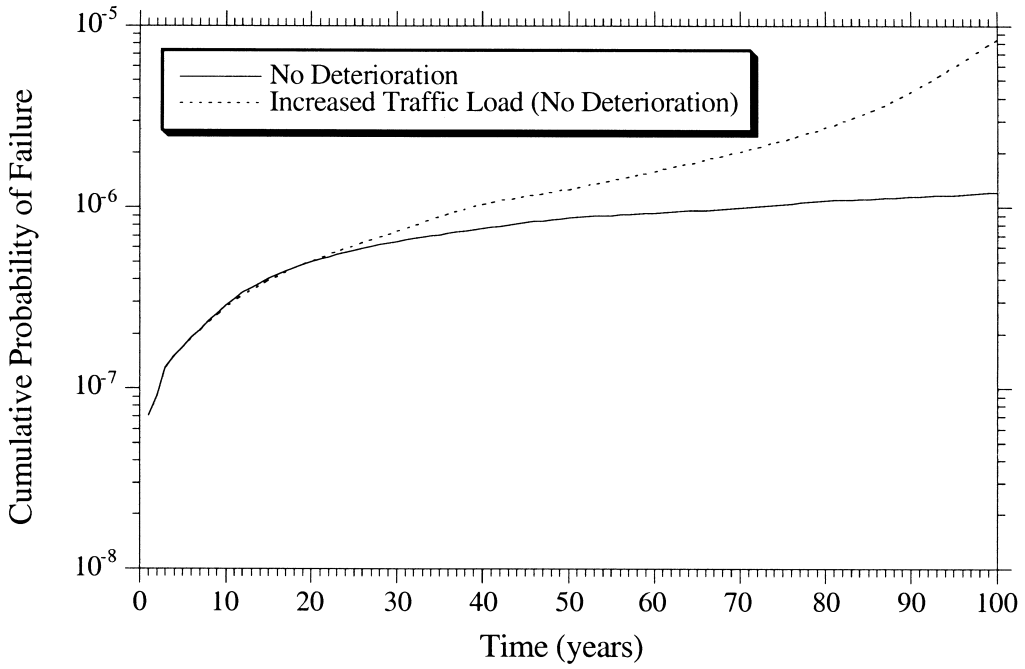

Fig. 11. Time-dependent cumulative probabilities of failure for increase in traffic loads [2.3% annual increase in traffic volume, traffic load (mass) increases by 0.5% per annum].

namely safety function $R-S$ where R is the ultimate strength and S is actual load effects. The relative sensitivity of each random variable i is estimated by considering each parameter to be a random variable whilst all other parameters are fixed at their mean values. Hence, the absolute influence of each random variable on the variability of the response variability (flexure or shear safety function) can be calculated in percentage terms (e.g. [48]); see Table 3 for safety functions (de-icing salts) at $t = 100$ years.

Table 3 shows that safety functions are mostly influenced by variabilities of steel yield stress (f_{sy}); truck loading; model errors for shear, flexure, C_o and D; concrete cylinder compressive strength (f'_{cyl}); and concrete top and bottom cover. The probability of structural failure also is most sensitive to the variability of these random variables. It follows that probabilities of structural failure may be reduced by reducing the variability of these random variables.

5. Accuracy of long-term predictions

Finally, long-term predictions of bridge performance are inherently uncertain since it is very difficult to predict with any degree of confidence long-term deterioration processes and increases in traffic loads and volume. Hence, predictions of the effect of deterioration processes on bridge performance can only be relatively accurate for relatively short time periods — say, for reference periods (time since previous assessment or updating) not exceeding 10 years. However, even over these short periods serviceability performance can change dramatically [4,5,9].

Table 3
Relative importance of variability of parameters on variability of strength limit state

Parameter	Flexure (%)	Shear (%)
Model error (D)	6.8	1.5
C_o	9.3	2.0
C_r	0.0	0.0
Model Error (i_{corr})	1.4	0.8
w_{max}	0.0	0.0
Critical crack width	0.0	0.0
Depth	3.5	1.0
C_{top}	14.3	3.7
C_{bottom}	9.1	2.2
f'_{cyl}	5.0	10.0
k_w ($f'_c = k_w f'_{cyl}$)	0.0	0.9
$f'_{ct}(t)$	0.0	0.0
$E_c(t)$	0.0	0.0
f_{sy}	19.5	0.0
Humidity	0.0	0.0
Shear strength model error	0.0	71.0
Flexure strength model error	7.9	0.0
Dead load	5.1	1.9
Asphalt load	0.6	0.2
Impact factor	0.6	0.4
Truck live load	11.3	6.3

6. Conclusions

An improved structural deterioration life-cycle reliability (probabilistic) model has been developed to calculate probabilities of structural failure. Three durability design specifications were considered in a lifetime reliability analysis of a RC slab bridge. Time-variant increases in loads were considered also. It was found that concrete cover and water–cement ratio have a large influence on probabilities of collapse. When compared to the case of "no deterioration", it was observed also that the probability of failure only marginally increased for good durability design specifications.

References

[1] Dunker KR, Rabbat BG. Why America's bridges are crumbling. Scientific American 1993;March:66–72.
[2] Hooks JM, Romack G. The tools of bridge management. In: Structural Engineering World Congress, San Francisco. Paper ref. T142-1. Elsevier Science (CDROM).
[3] Das PC. Development of a comprehensive structures management methodology for the highways agency. In: Das P, editor. Management of highway structures. London: Thomas Telford, 1999. p. 49–60.
[4] Stewart MG, Rosowsky DV. Time-dependent reliability of deteriorating reinforced concrete bridge decks. Structural Safety 1998;20(1):91–109.
[5] Stewart MG, Rosowsky DV. Structural safety and serviceability of concrete bridges subject to corrosion. ASCE Journal of Infrastructure Systems 1998;4:146–55.

[6] Bentz DP, Clifton JR, Snyder KA. Predicting service life of chloride-exposed steel-reinforced concrete. Concrete International 1996;18(12):42–7.
[7] CEB-FIP. Model code: design code. London: Comité Euro-International du Béton/Thomas Telford, 1990.
[8] Liu Y, Weyers RE. Time to cracking for chloride-induced corrosion in reinforced concrete. In: Page CL, Bamforth PB, Figg JW, editors. Corrosion of reinforcement in concrete construction. Cambridge (UK): Royal Society of Chemistry, 1996. p. 88–104.
[9] Stewart MG. Ongoing issues in time-dependent reliability of deteriorating concrete bridges. In: Das P, editor. Management of highway structures. London: Thomas Telford, 1999. p. 241–53.
[10] Tuutti K. Corrosion of steel in concrete. Stockholm: Swedish Cement and Concrete Research Institute, 1982.
[11] HETEK. A system for estimation of chloride ingress into concrete: theoretical background. Report no. 83, The Danish Road Directory, 1997.
[12] Middleton CR, Hogg V. Review of deterioration models used to predict corrosion in reinforced concrete structures (CUED/D — STRUCT/TR.173). Cambridge University, 1998.
[13] Hoffman PC, Weyers RE. Predicting critical chloride levels in concrete bridge decks. In: Schueller GI, Shinozuka M, Yao JTP, editors. Structural Safety and Reliability: Proceedings of ICOSSAR'93. Rotterdam: A.A. Balkema, 1994. p. 957–9.
[14] Neville A. Chloride attack of reinforced concrete: an overview. Materials and Structures 1995;28:63–70.
[15] Berke NS, Hicks MC. In: Charker V, editor. The life cycle of reinforced concrete decks and marine piles using laboratory diffusion and corrosion data, corrosion forms and control for infrastructures (ASTM STP 1137). Philadelphia: American Society for Testing and Materials, 1992. p. 207–31.
[16] Ohta T. Corrosion of reinforcing steel in concrete exposed to sea air. In: Malhotra VM, editor. Durability of concrete (ACI SP-126). Detroit: American Concrete Institute, 1991. p. 459–77.
[17] Uji K, Matsuoka Y, Maruya T. Formulation of an equation for surface chloride content of concrete due to permeation of chloride. In: Page CL, Treadway KWJ, Bamforth PB, editors. Corrosion of reinforcement in concrete. Barking (UK): Elsevier Science, 1990. p. 258–67.
[18] Takewaka K, Mastumoto S. Quality and cover thickness of concrete based on the estimation of chloride penetration in the marine environments. In: Malhotra VM, editor. Concrete in marine environment (ACI SP-109). Detroit: American Concrete Institute, 1988. p. 381–400.
[19] Bamforth PB, Price WF. An international review of chloride ingress into structural concrete. Report no. 1303/96/9092. Taywood Engineering Ltd Technology Division, 1997.
[20] McGee R. Modelling of durability performance of tasmanian bridges. In: Melchers RE, Stewart MG, editors. ICASP8 applications of statistics and probability in civil engineering, vol. 1, 1999. p. 297–306.
[21] HETEK. Chloride penetration into concrete — state of the art. Report no. 53. The Danish Road Directory, 1996.
[22] Cabrera JG, Dodd TAH, Nwaubani SO. The effect of curing temperarure on the chloride ions diffusion of super plasticised cement and fly ash cement pastes. In: Maclnnis C, editor. Durable concrete in hot climates (SP-139). ACI, 1993. p. 61–76.
[23] Hobbs DW. Minimum requirements for durable concrete: carbonation- and chloride-induced corrosion, freeze-thaw attack and chemical attack. Crowthorn (UK): British Cement Association, 1998.
[24] Lin SH. Chloride diffusion in a porous concrete slab. Corrosion 1990;46(12):964–7.
[25] Papadakis VG, Roumeliotis AP, Fardis MN, Vagenas CG. Mathematical modelling of chloride effect on concrete durability and protection measures. In: Dhir RK, Jones MR, editors. Concrete repair, rehabilitation and protection. London (UK): E&FN Spon, 1996. p. 165–74.
[26] Suzuki M, Tsutsumi T, Irie M. Reliability analysis of durability/deterioration indices of reinforced concrete in a marine environment. In: Page CL, Treadway KWJ, Bamforth PB, editors. Corrosion of reinforcement in concrete. Barking (UK): Elsevier Science, 1990. p. 381–400.
[27] Matsushima M, Tsutsumi T, Seki H, Matsui K. A study of the application of reliability theory to the design of concrete cover. Magazine of Concrete Research 1998;50(1):5–16.
[28] Yalsyn H, Ergun M. The prediction of corrosion rates of reinforcing steels in concrete. Cement and Concrete Research 1996;26(10):1593–9.
[29] Libby JR. Modern prestressed concrete: design principles and construction methods. New York: Chapman and Hall, 1990.

[30] Hui HD, Strekalov PV, Kikhailovskii YN, Bin DT, Mikhailov AA. The corrosion resistance of steels, zinc, copper, aluminium, and alloys in the humid tropics of Vietnam. The results of five-year tests. Protection of Metals 1994;30(5):437–43.
[31] Yokozeki K, Motohashi K, Okada K, Tsutsumi T. A rational model to predict the service life of RC structures in a marine environment. In: Fourth CANMET/ACI International Conference on Durability of Concrete (SP 170-40), 1997. p. 778–99.
[32] Liu T, Weyers RE. Modeling the dynamic corrosion process in chloride contaminated concrete structures. Cement and Concrete Research 1998;28(3):365–79.
[33] Thoft-Christensen P. Advanced bridge management systems. Structural Engineering Review 1995;7(3):151–63.
[34] Frangopol DM, Lin K-Y, Estes AC. Reliability of reinforced concrete girders under corrosion attack. Journal of Structural Engineering, ASCE 1997;123(3):286–97.
[35] Val D, Stewart MG, Melchers RE. Effect of reinforcement corrosion on reliability of highway bridges. Engineering Structures 1998;20(11):1010–9.
[36] Rodriguez J, Ortega LM, Casal J. Load carrying capacity of concrete structures with corroded reinforcement. Construction and Building Materials 1997;11(4):239–48.
[37] Ellingwood B, Mori Y. Reliability-based service life assessment of concrete structures in nuclear power plants: optimum inspection and repair. Nuclear Engineering and Design 1997;175:247–58.
[38] Stewart MG, Val D. Role of load history in reliability-based decision analysis of ageing bridges. Journal of Structural Engineering, ASCE 1999;125(7):776–83.
[39] Kameda H, Koike T. Reliability analysis of deteriorating structures. In: Reliability approach in structural engineering. Tokyo: Maruzen Co., 1975. p. 61–6.
[40] Mori Y, Ellingwood BR. Reliability-based service-life assessment of aging concrete structures. Journal of Structural Engineering, ASCE 1993;119(5):1600–21.
[41] Nowak AS. Live load models for highway bridges. Structural Safety 1993;13:53–66.
[42] AASHTO-LRFD. AASHTO LRFD bridge design specifications. Washington (DC): Association of State Highway and Transportation Officials, 1994.
[43] ACI318. Building code requirements for structural concrete. Detroit (MI): American Concrete Institute, 1995.
[44] ACI 209. Prediction of creep, shrinkage and temperature effects: 2. ACI Committee 209, 1978.
[45] Micic TV, Chryssanthopoulos MK, Baker MJ. Reliability analysis for highway bridge deck assessment. Structural Safety 1995;17:135–50.
[46] ICE. Managing the highways network. London: The Institution of Civil Engineers, 1994.
[47] Brown JH. The performance of concrete in practice: a field study of highway bridges. TRRL Contractor Report no. 43, 1987.
[48] Novak D, Teply B, Kersner Z. The role of latin hypercube sampling method in reliability engineering. In: Shiraisha N, Shinozuka M, Wen YK, editors. Proceedings of ICOSSAR'97 — Seventh International Conference on Structural Safety and Reliability, vol. 1. Rotterdam: A.A. Balkema, 1998. p. 403–9.